

See discussions, stats, and author profiles for this publication at: <https://www.researchgate.net/publication/283122552>

# Bimodal Latex Effect on Spin Coated Thin Conductive Polymer SWCNT Layers

ARTICLE *in* LANGMUIR · OCTOBER 2015

Impact Factor: 4.46 · DOI: 10.1021/acs.langmuir.5b02756

---

READS

44

## 8 AUTHORS, INCLUDING:



Mohammad-Amin Moradi  
Technische Universiteit Eindhoven

3 PUBLICATIONS 1 CITATION

[SEE PROFILE](#)



Karthikeyan Gnanasekaran  
Technische Universiteit Eindhoven

9 PUBLICATIONS 93 CITATIONS

[SEE PROFILE](#)



Heiner Friedrich  
Technische Universiteit Eindhoven

66 PUBLICATIONS 1,612 CITATIONS

[SEE PROFILE](#)



Alex M. van Herk  
Technische Universiteit Eindhoven

218 PUBLICATIONS 3,971 CITATIONS

[SEE PROFILE](#)

## Bimodal Latex Effect on Spin-Coated Thin Conductive Polymer–Single-Walled Carbon Nanotube Layers

Mohammad-Amin Moradi,<sup>†</sup> Katalin Larrakoetxea Angoitia,<sup>†</sup> Stefan van Berkel,<sup>§</sup> Karthikeyan Gnanasekaran,<sup>†</sup> Heiner Friedrich,<sup>†</sup> Johan P. A. Heuts,<sup>†</sup> Paul van der Schoot,<sup>‡,||</sup> and Alex M. van Herk<sup>\*,†,‡</sup>

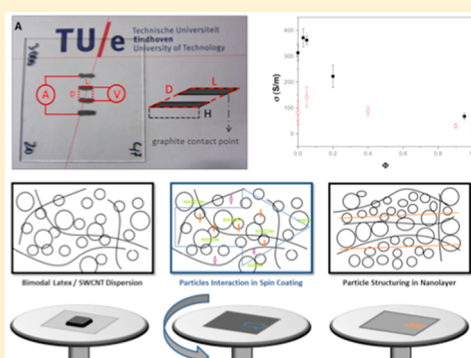
<sup>†</sup>Department of Chemical Engineering and Chemistry and <sup>‡</sup>Department of Applied Physics, Eindhoven University of Technology, P.O. Box 513, 5600 MB, Eindhoven, The Netherlands

<sup>§</sup>Polymer Technology Group Eindhoven B.V. (PTG/e), P.O. Box 6284, 5600 HG, Eindhoven, The Netherlands

<sup>||</sup>Institute for Theoretical Physics, Utrecht University, Leuvenlaan 4, 3584 CE Utrecht, The Netherlands

<sup>\*</sup>Institute of Chemical and Engineering Sciences, 1 Pesek Road, Jurong Island 627833, Singapore

**ABSTRACT:** We synthesize two differently sized poly(methyl methacrylate-*co*-*tert*-butyl acrylate) latexes by emulsion polymerization and mix these with a sonicated single-walled carbon nanotube (SWCNT) dispersion, in order to prepare 3% SWCNT composite mixtures. We spin-coat these mixtures at various spin-speed rates and spin times over a glass substrate, producing a thin, transparent, solid, conductive layer. Keeping the amount of SWCNTs constant, we vary the weight fraction of our smaller 30-nm latex particles relative to the larger 70-nm-sized ones. We find a maximum in the electrical conductivity up to 370 S/m as a function of the weight fraction of smaller particles, depending on the overall solid content, the spin speed, and the spin time. This maximum occurs at 3–5% of the smaller latex particles. We also find a more than 2-fold increase in conductivity parallel to the radius of spin-coating than perpendicular to it. Atomic force microscopy points at the existence of lanes of latex particles in the spin-coated thin layer, while large-area transmission electron microscopy demonstrates that the SWCNTs are aligned over a grid fixed on the glass substrate during the spin-coating process. We extract the conductivity distribution on the surface of the thin film and translate this into the direction of the SWCNTs in it.



### INTRODUCTION

Carbon nanotubes (CNTs) have attracted a great deal of interest since the study of arc-discharge fabricated CNTs published by Iijima in 1991.<sup>1</sup> Carbon nanotubes exhibit unique electrical, optical, and mechanical properties, alone and in a composite.<sup>2</sup> For example, the tensile strength and Young's modulus of a single-walled carbon nanotube (SWCNT) are estimated to be 37 and 640 GPa, respectively, while the electrical conductivities of SWCNT ropes are  $(1\text{--}3) \times 10^6$  S/m.<sup>3–5</sup> The choice of carbon nanotube filler particles to prepare conductive polymeric composites is a sensible one, due to their superior electrical properties and potentially very low percolation threshold. This means that minimal loading is required to achieve significant conductivity.<sup>6–9</sup> Coatings and films have been produced to give rise to conductivities of around 700 S/m of 2–10% CNT-containing transparent films.<sup>10</sup> The mixtures are easily processed and are of interest for a wide range of potential electronic applications, including display technologies, flexible electronics, optoelectronic devices, and smart labels and sensors.<sup>11–14</sup>

CNTs can be incorporated into insulating polymers to make conductive composites by a variety of preparation techniques, including ball-milling, melt-mixing, slot-die-coating, and spin-

coating, but most of them suffer from limitations in film homogeneity and thickness control.<sup>15–18</sup> Meanwhile, some researchers have tried to use solvent-based latex particle dispersions as a starting point for producing thin films and achieving an improved assembly of carbon nanotubes in a conductive network and lower percolation threshold.<sup>19,20</sup> In this so-called latex technology, small latex particles are mixed with ultrasonicated CNTs in a suitable solvent, where the large size difference of the CNTs and the latex particles are thought to aid the assembly of CNTs during the production of the final solid film.<sup>21,22</sup> Indeed, film formation of mixtures of latex particles and carbon nanotubes often results in a more highly conductive composite film and reduced percolation threshold, which has been explained in terms of so-called depletion interactions between the CNTs due to the presence of the much smaller latex particles.<sup>23</sup>

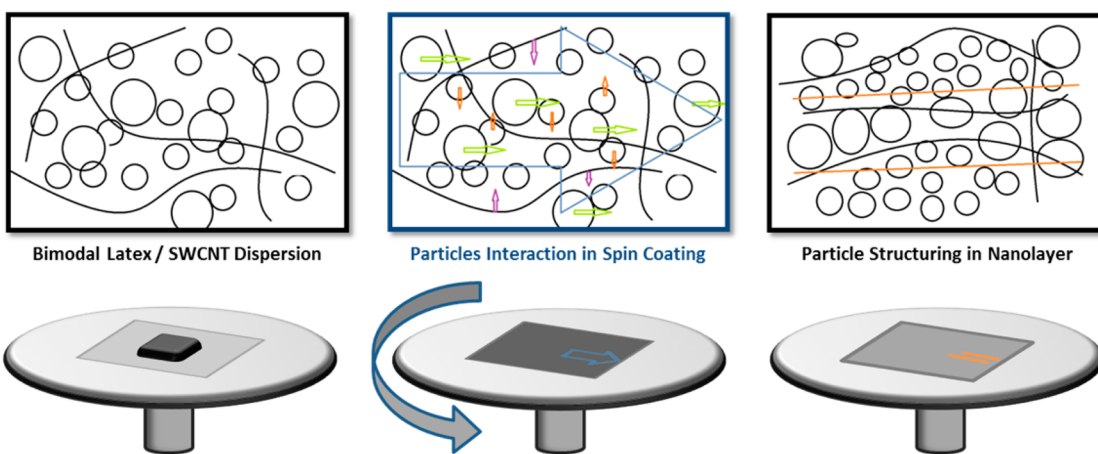
In this work, we aim to improve the quality of the CNT network and through that the conductivity of thin-film composites by using film-forming mixtures of differently sized

Received: July 30, 2015

Revised: October 2, 2015

Published: October 22, 2015

**Scheme 1.** Schematic Illustration of the Local Structuring of SWCNT–Latex Mixtures Resulting from the Spin-Coating Procedure<sup>a</sup>



<sup>a</sup>The structuring is arguably caused by the phase separation of the mixture and the concomitant lane formation of the particles that in turn enhances the alignment of the SWCNTs in the final solid product.

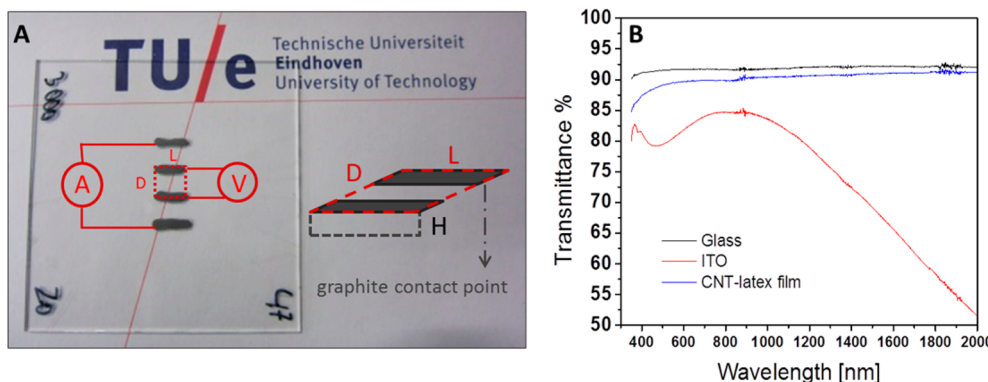


**Figure 1.** (A) Spin-coated SWCNT–latex dispersion on a glass surface heated above MFFT = 44 °C for 15 min and prepared for conductivity measurements. (B) Transmittance of glass, glass coated with ITO, and glass coated with the SWCNT–latex mixture in the wavelength range from 350 to 2000 nm.

latex particles and SWCNTs and subjecting them to a horizontal centrifugal force through spin-coating (Scheme 1).<sup>24,25</sup> Our approach is inspired by studies of mixtures of colloidal particles of different sizes and shapes that under flow respond differently to hydrodynamic forces. This could give rise to oriented clusters of rod-shaped particles, driven by the interaction with the spherical particles in the dispersion that tend to form lanes.<sup>26,27</sup> We investigate whether applying a mixture of differently sized colloidal particles, which themselves tend to segregate, aids in obtaining oriented lane formation and localization of CNTs in the mixture.<sup>28</sup> We expect this effect to result in a higher conductivity of the coating.

## EXPERIMENTAL SECTION

To prepare the nanoscale SWCNT–poly(methyl methacrylate-*co*-*tert*-butyl acrylate) [p(MMA-*co*-t-BA)] films, we sonicated an aqueous SWCNT dispersion using a 750 W Vibra-cell (model CV33) tip sonication device—as described by Yu et al.<sup>22</sup>—for 3 h at 30% power. Our SWCNTs were purchased from Carbon Nanotechnologies Inc. and are currently known as Unidym (CNI Lot # PO 257). The solution also contained sodium dodecyl sulfate (SDS) from Merck (2011), and we used deionized water to obtain a well-dispersed SWCNT dispersion (44 mg of SWCNT, 88 mg of SDS, and 20 g of water). In order to obtain the desired solid content of 4–5 w/w%, we mixed our SWCNT dispersions with in-house synthesized latexes of

30- and 70-nm-sized particles, made of 99% pure methyl methacrylate (MMA) and 98% pure *tert*-butyl acrylate (t-BA) from Aldrich. We prepared our latexes by starved-feed emulsion polymerization of a [MMA]/[t-BA] = 3 monomer mixture with solid content of 20% in 5 h with a minimum film formation temperature (MFFT) of about 44 °C. This prevents the flow of polymer material around room temperature out of the desired particle assembly in our latex-based route of preparing SWCNT composites.<sup>15,31</sup>

Several mixtures of SWCNT and latex (up to 5% solid content) were spread over a 3 × 3 cm<sup>2</sup> area on the glass substrate using a Pasteur pipet and immediately spin-coated via a Karl Suss model CT62 spin-coater at various speeds in the range from 1000 to 4000 rpm, for 20–40 s. We set the acceleration of spin-coating at 500 (rs<sup>-2</sup>) for all of the samples. Finally, we obtained the conductivity of each film by a four-point, direct current conductivity measurement, using a Keithley model 273 electrometer, applying a current over the sample, and a Keithley model 6517A electrometer, measuring the resulting voltage drop between the electrodes.

We applied carbon electrodes on the surface of the coating, ensuring good contact and defining the measurement geometry. This also prevents surface effects from interfering with our measurements. The carbon electrodes were prepared by using a graphite dispersion from Electron Microscopy Sciences (cat. #12660) and applying this in four parallel lines of length L = 5 mm with a spacing D of 5 mm between them, as shown in Figure 1A.<sup>23</sup> Relying on spectrophotometry to establish the transparency of the typical spin-coated glass by our prepared SWCNT–latex mixtures, we find it to be about 97%

of that of the glass substrate at 520 nm wavelength, a value that does not seem to drop for wavelengths up to 2000 nm. As shown in Figure 1B, this is clear in contrast with our measurements on a indium–tin oxide (ITO) coated glass slide (CAS No. 50926-11-9), measured by a UV-vis-IR scanning spectrophotometer (UV-3102 PC), the transmittance of which does drop significantly for larger wavelengths.

The conductivity ( $\sigma$ ) of the films was determined by varying the current ( $I$ ) over the sample in the range from nanoamperes to microamperes, and the resulting voltage ( $U$ ) over the measurement area was measured, taking into account the measurement distance ( $L$ ) and thickness ( $H$ ) of the sample. For this purpose we made use of the expression<sup>9</sup>

$$\sigma = \frac{D}{LH\frac{U}{I}} \quad (1)$$

To measure the thickness ( $H$ ) of the film accurately, we removed part of the coating using a razor blade and created a clear edge. The height difference between the coating and the glass surface could then accurately be determined by a Zoumsurf 3D optical profilometer (Fogale).

## RESULTS AND DISCUSSION

We investigated the effect of bimodality in the latex particle size using mixtures of 30- and 70-nm-sized latex particles in the production of our SWCNT-latex nanolayers for a host of spin-coating conditions. Figure 2 shows the effect of the duration

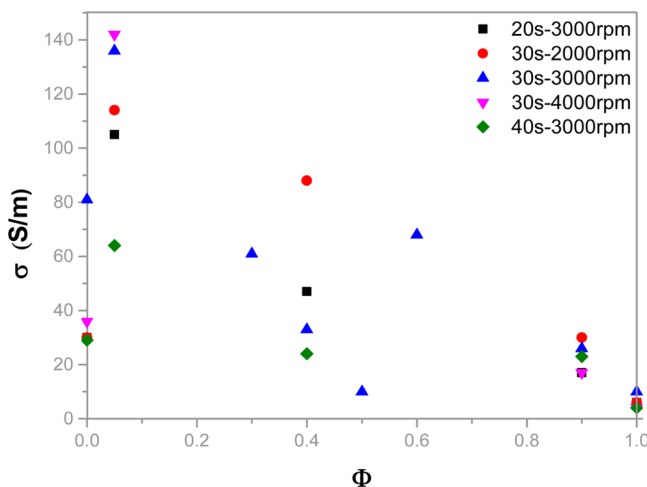


**Figure 2.** Effect of composition, spin-coating speeds, and duration on the conductivity ( $\sigma$ ) of the composite nanolayers. Indicated on the horizontal axis is the volume fraction ( $\Phi$ ) of the 30-nm latex particles relative to the 70-nm ones.

and speed of the spin-coating on the conductivity of the film as a function of the volume fraction ( $\Phi$ ) of the smaller latex relative to the overall volume fraction of particles. The experiments were carried out at 5% solid content in the fluid preparation phase of the composite, following earlier studies on coating nanometer-sized latex on a glass substrate.<sup>32</sup>

It is clear from Figure 2 that the relation between the fraction of 30-nm latex particles and the conductivity is highly nonlinear and indicative of what has been dubbed *synergetic percolation*.<sup>22</sup> Indeed, the addition of small amounts of 30-nm latex particles to the 70-nm ones leads to a larger conductivity than using either size alone, and a clear maximum is exhibited. It hints at a complex arrangement of CNTs within the composite film caused by interactions with the latex particles when still in the fluid dispersion state.<sup>22</sup> Note also that the conductivity of the

samples prepared with only the 70-nm latex particles (so with zero fraction of smaller latex particles,  $\Phi = 0$ ) is larger than that of the samples prepared with the 30-nm latex particles ( $\Phi = 1$ ). This is to be expected theoretically on account of the fact that larger latex particles induce stronger attractive depletion interactions between the CNTs in the fluid preparation stages of the composite.<sup>22</sup> It is not clear why the spin-coating conditions have such a significant and complex impact on the conductivity of the final product: increasing the spin speed may either increase or decrease the conductivity of the composite, depending on the fraction of smaller particles. A clear trend can however not be discerned.

We also performed experiments at a lower level of 4% solid content in the fluid dispersion. At each fraction of the smaller (30 nm) latex particles, we applied different spin-coating conditions to find the optimum, that is, largest, conductivity. As Figure 3 shows, we find a clear improvement in the overall

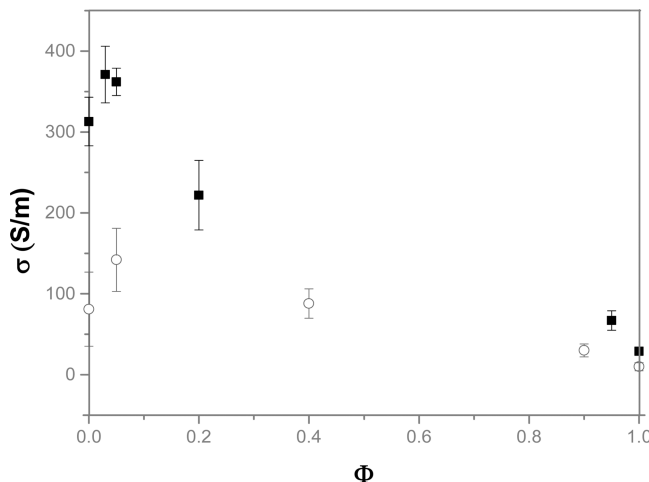


**Figure 3.** Effect of the fraction of the smaller latex ( $\Phi$ ) on conductivity ( $\sigma$ ) under optimal processing conditions of spin speed and time for 5% and 4% solid contents. The amount of SWCNT in all solid samples is 3 wt %. The total solid content in the fluid dispersion before spin-coating is 5% (○) and 4% (■), respectively.

conductivity when compared to our findings using the 5% solid content mixture. (Note the different conductivity scale of Figure 3 versus that in Figure 2.) Again we find that there is an increase in conductivity upon adding a small amount of the smaller latex particles to the 70-nm latex particles. The effect is actually more pronounced at the lower than at the somewhat higher solid fraction concentration. It remains unclear why a small change in solid fraction of 20% has such a large effect. It is evident from our results that there is no one set of processing conditions that leads to maximum conductivity for all compositions  $\Phi$ . The optimal conditions are listed in Table 1.

It seems reasonable to presume that the complex response of the conductivity of the films on the composition and spin-coating conditions must somehow be connected with how the various types of particles respond to these conditions. In order to get insight into this, we prepared samples with the optimum conductivities for transmission electron microscopy (TEM) and atomic force microscopy (AFM) studies. Figure 4 shows the particle arrangement before spin-coating (A), after spin-coating (B), and after heating the spin-coated film to 60 °C for 15 min (C). There is a clear indication of alignment in the particle arrangement in the AFM image 4B. The presence of

**Table 1. Conductivity of the Final Solid Film under Optimum Processing Conditions for Different Fractions of 30- and 70-nm Latex Particles in Mixture**

5% solid content				4% solid content			
$\Phi_{30}$	time (s)	rpm	$\sigma$ (S/m)	$\Phi_{30}$	time (s)	rpm	$\sigma$ (S/m)
0.00	30	3000	81	0.00	40	3000	313
0.05	30	4000	142	0.03	30	4000	371
0.40	30	2000	88	0.05	20	3000	362
0.90	30	2000	30	0.20	20	3000	222
1.00	20	3000	10	0.95	30	4000	67
			1.00	40	3000		29

oriented lanes of latex particles suggested that the SWCNT network must be aligned, too, and therefore, the conductivity of the film must be different in different directions.

Because of the geometry of the spin-coating process, we expect radial flow fields in the fluid dispersion that by themselves should lead to a radial alignment of the SWCNTs. Plausibly, this alignment effect is strengthened by lane formation of the colloids that should follow the same radial geometry. In order to investigate this hypothesis, we performed orientation conductivity measurements. Results of these measurements are presented in Figure 5.

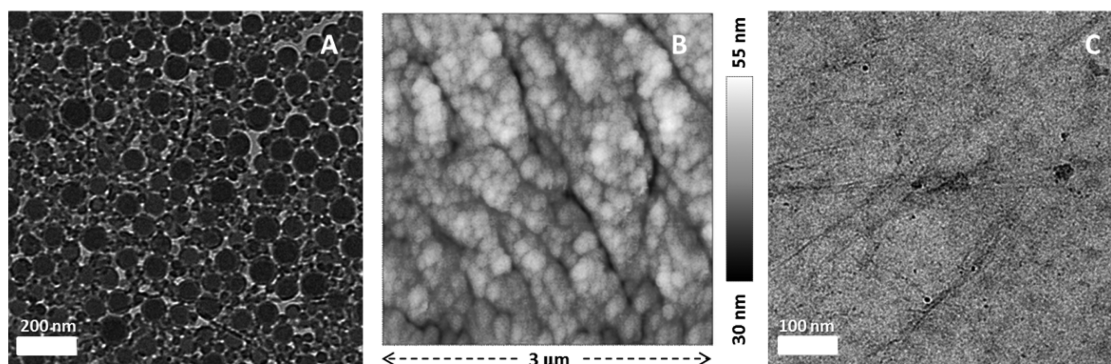
Three samples were prepared and spin-coated under identical conditions. The four-point direct-current conductivity measurements allowed us to investigate the anisotropy of the conductivity as a function of the distance from the center of spin-coating. We find, for example, the highest conductivity of 150 S/m for configuration iii in Figure 5A, which is about 2 times the conductivity of 82 S/m in configuration viii of Figure 5B in the same radial orientation of the measurement, but further away from the center. It is 5 times that of configuration C(xi), which is almost the same distance from the center of spin-coating but where the conductivity was measured at right angles to the radial direction. Radial measurements at the same distance from the spinning center give similar but not identical values of the conductivity. See configurations vi–ix of Figure 5B. This indicates (a) that the conductivity is larger along the radial direction than perpendicular to that, presumably because of the alignment of the SWCNTs, and (b) that the spatial distribution of SWCNTs may not be uniform.

More detailed information on the conductivity ( $\sigma$ ) over the entire surface of the film may be obtained by measuring  $\sigma$  as a function of the distance ( $r$ ) to the center of the spin-coating

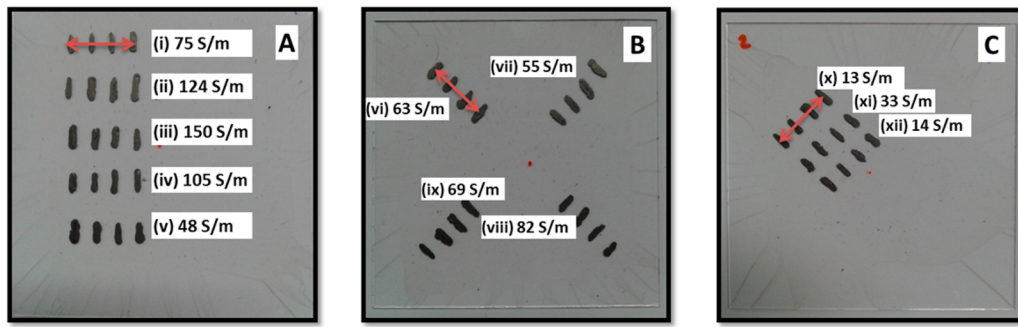
and the angle  $\theta$  between the main axis of the row of electrodes relative to the vector connecting the spin-coating center and the measurement position. See Figure 6A. This allows us to collect spatially and angularly resolved conductivities ( $\theta, r, \sigma$ ) that we indicate by specifying the corresponding coordinates. Results are collected in Figure 6B, where  $r$  varies from 0 cm (the center of spin-coating) to almost 2 cm (near to the edge of the continuous film) and the measurement angle  $\theta$  varies from 0° to 90°. Indicated in the figure are also the configurations A(ii,iii), B(vii), and C(xi) of Figure 5.

Figure 6B confirms that, generally speaking, the conductivity drops (i) if we move away from the spin center of the film and (ii) if the measurement angle increases away from perfect radial alignment. However, there are also less obvious trends that cannot be reconciled with our naïve expectation of perfect radial symmetry. Indeed, the maximum conductivity is around  $(\theta, r, \sigma) = (5.3^\circ, 0.9 \text{ cm}, 150 \text{ S/m})$ . The conductivity drops to less than half of the maximum, moving from  $(5.3^\circ, 0.9 \text{ cm}, 150 \text{ S/m})$  to  $(10^\circ, 1.49 \text{ cm}, 55 \text{ S/m})$ . It clearly decreases below one-third of the maximum value when the angle  $\theta$  is larger than 60°, regardless of the radial distance  $r$  from the center of the sample. There is another maximum of conductivity around  $(42.7^\circ, 1.31 \text{ cm}, 124 \text{ S/m})$ , and the line between  $(5.3^\circ, 0.9 \text{ cm}, 150 \text{ S/m})$  and  $(42.7^\circ, 1.31 \text{ cm}, 124 \text{ S/m})$  is a line of locally connected maxima in the conductivity on the surface of the film. These actually represent a saddle point region between points ii and iii and is indicated by the dashed line.

From Figure 6B, we are able to deduce a conductivity landscape, represented schematically in Figure 7A,B. Although generally the geometry is radial, there are deviations from perfect radial alignment that we speculate must be connected with the deviations of a purely radial fluid flow during spin-coating caused by the spreading of the flow over the surface. As a consequence, although the conductivity drops with the measurement position moving away from the center in line with the reduction of SWCNT density in the spin-coated film, the direction of maximum conductivity increases from close to 0° to no less than 40°. It is not evident from the measurements themselves, but it is not unlikely that the deviation of the maximum conductivity direction from radial to 40° not being radially symmetric is caused by processes relating to the spin-coating direction (clockwise vs counterclockwise).<sup>25</sup> It could be due to effects resulting from the presence of the edges causing gradients in the velocities of the particles over the film at different radial distances from the center of spin-coating.



**Figure 4.** TEM images of the latex–CNT mixture before (A) and after (C) processing. In between these two panels, B shows an AFM image of a not heated spin-coated mixture, which is representative of particle arrangement before the final heating step. SWCNTs are continuous dark lines in panels A and C. Spin-coating was done at 3000 rpm for 30 s, and sample C was heated to 60 °C for 15 min.



**Figure 5.** Directional measurement of the electrical conductivity on three samples prepared under identical conditions. The conductivity was measured at 12 different points by the four-point technique. The maximum conductivity of the same prepared samples is found in configuration A(iii) at 150 S/m and the minimum in configuration C(x) at 13 S/m.

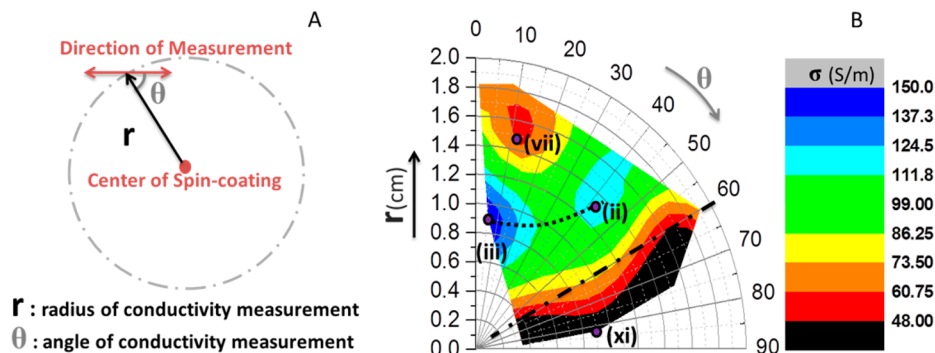


**Figure 6.** Data analysis on spin-coated composite films shows a pattern of conductivity over the nanolayer. In the range of the correlated data, it is shown that conductivity falls off at  $\theta$  values of over 60°.

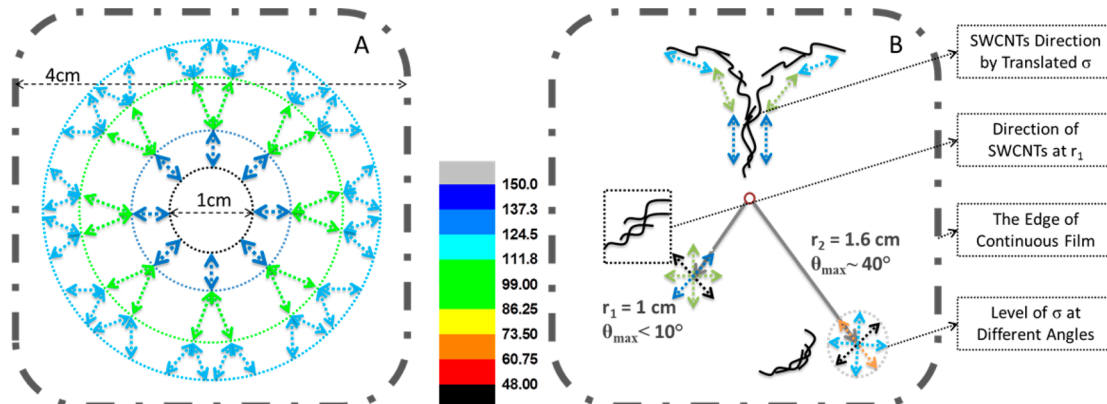


**Figure 7.** (A) Pattern of maximum conductivity in the composite film deduced from Figure 6. (B) Translation of maximum conductivity pattern in terms of the orientation of the SWCNTs in the film.

Specifically, the slight increase of the conductivity from (35°, 1.1 cm, 105 S/cm) to (42.7°, 1.31 cm, 124 S/cm) may well be caused by some as yet poorly understood mechanism preventing spreading SWCNTs close to the edge of the film. This mechanism is currently under investigation, and results shall be reported elsewhere.

Presuming that the majority of the conductive elements are oriented in parallel with the maximum conductivity direction, we expect a gradual change in the orientation of SWCNTs at 1–1.6 cm distance away from the spin-coating center (Figure 7B). However, from the TEM images that we have taken and that we present in Figure 8, it seems that the orientations of the carbon nanotubes slightly change from largely radial to different

angles relative to the radial direction when approaching the less dense areas on the surface of the continuous film.

## CONCLUSIONS

We find that the composition of particle sizes in a binary latex mixture affects the conductivity of a spin-coated SWCNT–latex film. For a binary latex system containing a mixture of 30- and 70-nm latex particles, the best results are achieved with 3–5% of the 30-nm latex particles ( $\Phi = 0.03–0.05$ ) added to the 70-nm ones. Arguably, this is an example of synergetic percolation,<sup>23</sup> because the lower the percolation threshold, the larger the conductivity at a given filler fraction. Interestingly, the conductivity increases when the solid content of the mixture in the fluid dispersion stages of the film

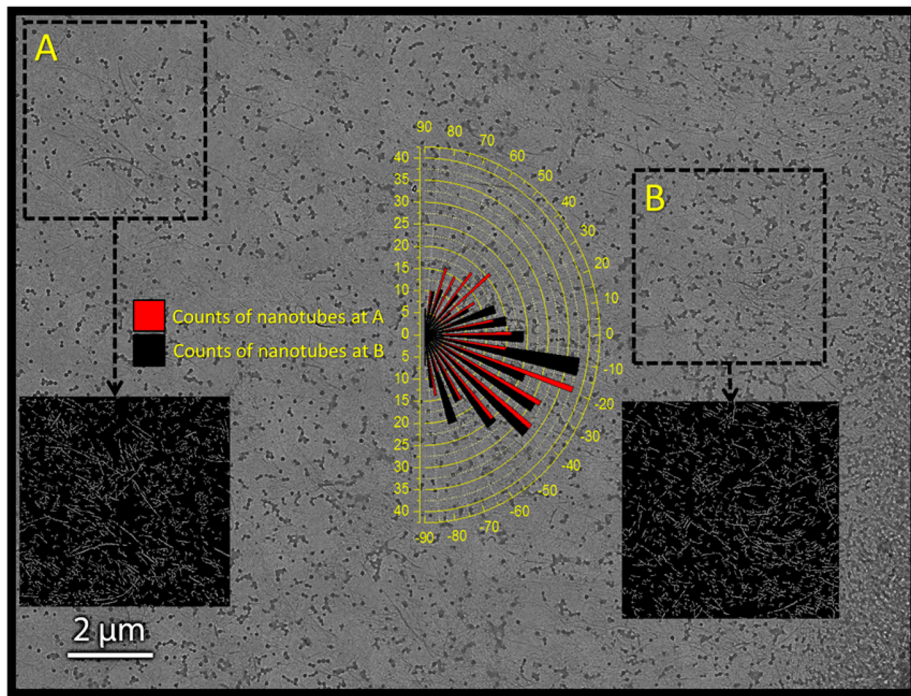


**Figure 8.** Large-area TEM over a 200 mesh copper grid placed on the substrate at 1.2 cm from the spin-coating center to investigate any changes of the orientation of the SWCNTs with lateral position in the film. The bias of orientation away from 0° could be caused by the position of the grid over the substrate, different flow regimes of the material on the surface during spin-coating, or the effect of the spin-coating direction.

production, which includes 3 w/w% SWCNT and 97 w/w% polymer, is reduced from 5 to 4 w/w%.

Compared to the pure 70-nm latex particles case ( $\Phi = 0$ ), the conductivity rise is 10% when the 4% solid content system is applied, while it is 50% at 5% solid content. The larger conductivity difference at higher solid content could be caused by stronger interactions between the latex particles at higher concentrations. We find that the conductivity of the film spin-coated with only the 70-nm latex particles is more than twice that using the 30-nm latex particles at 5% solid content and about 5 times that at 4% solid content. This most likely is due to the stronger depletion interactions at higher solid content. The 30-nm monomodal latex-SWCNT spin-coated film produces the lowest conductivity, being at least 1 order of magnitude lower than the suitable mixture of size designed, binary latex.

Conductivities are about 3 times larger parallel to the spin-coating radius rather than perpendicular to it. This is true all over the studied surface area, implying that there must be a net orientation in the conductive network, plausibly caused by centrifugal flow fields during spin-coating and hydrodynamic interactions leading to lane formation of the filler particles. The maximum conductivity of the surface is obtained at a certain distance from the center of spin-coating and along the radial direction, presumably because migration of particles away from the center causes a lowering of the SWCNT density away from the center toward the rim of the spin-coated surface. Different mechanisms of dispersion flow during spin-coating seem to produce a direction-changing pattern of the conductive network in the film, which needs to be further studied. The spin-coating process of conductive filler-designed latex dispersions is complex but in principle controllable. A better understanding of it can help in the discovery of an optimal geometry for conductive networks in thin, flexible films.

## ■ AUTHOR INFORMATION

### Corresponding Author

\*E-mail: a.m.v.herk@tue.nl.

### Notes

The authors declare no competing financial interest.

## ■ ACKNOWLEDGMENTS

The authors thank Marco Hendrix for support on the AFM imaging and acknowledge the DPI Value Center for assistance in basic training in carbon nanotube composite preparation via the latex-based route.

## ■ REFERENCES

- (1) Iijima, S. Helical microtubules of graphitic carbon. *Nature* **1991**, *354* (6348), 56–58.
- (2) Shim, B. S. Multifunctional Carbon Nanotube Thin Film Composites by Layer-by-Layer Assembly Technique. Ph.D. Thesis, University of Michigan, Ann Arbor, MI, 2009.
- (3) Baughman, R. H.; Zakhidov, A. A.; de Heer, W. A. Carbon nanotubes—the route toward applications. *Science* **2002**, *297* (5582), 787–92.
- (4) Yu, M.; Files, B.; Arepalli, S.; Ruoff, R. Tensile loading of ropes of single wall carbon nanotubes and their mechanical properties. *Phys. Rev. Lett.* **2000**, *84* (24), 5552–5.
- (5) Thess, A.; Lee, R.; Nikolaev, P.; et al. Crystalline Ropes of Metallic Carbon Nanotubes. *Science* **1996**, *273* (5274), 483–7.
- (6) Cao, J. X.; Yan, X. H.; Ding, J. W.; Wang, D. L.; Lu, D. Electronic Properties of Single-Walled Carbon Nanotubes. *J. Phys. Soc. Jpn.* **2002**, *71* (5), 1339–45.
- (7) Guo, J.; Liu, Y.; Prada-Silvy, R.; et al. Aspect ratio effects of multi-walled carbon nanotubes on electrical, mechanical, and thermal properties of polycarbonate/MWCNT composites. *J. Polym. Sci. Part B Polym. Phys.* **2013**, *52*, 73–83.
- (8) Rahatekar, S. S.; Hamm, M.; Shaffer, M. S. P.; Elliott, J. A. Mesoscale modeling of electrical percolation in fiber-filled systems. *J. Chem. Phys.* **2005**, *123* (13), 134702.

- (9) Hermant, M. C.; Klumperman, B.; Kyrylyuk, A. V.; van der Schoot, P.; Koning, C. E. Lowering the percolation threshold of single-walled carbon nanotubes using polystyrene/poly(3,4-ethylenedioxothiophene): poly(styrene sulfonate) blends. *Soft Matter* **2009**, *5* (4), 878.
- (10) Zhang, D.; Ryu, K.; Liu, X.; et al. Transparent, conductive, and flexible carbon nanotube films and their application in organic light-emitting diodes. *Nano Lett.* **2006**, *6* (9), 1880–1886.
- (11) Sirringhaus, H.; Tessler, N.; Friend, R. Integrated optoelectronic devices based on conjugated polymers. *Science* **1998**, *280* (5370), 1741–4.
- (12) Denneulin, A.; Blayo, A.; Bras, J.; Neuman, C. PEDOT:PSS coating on specialty papers: Process optimization and effects of surface properties on electrical performances. *Prog. Org. Coat.* **2008**, *63* (1), 87–91.
- (13) Sainz, R.; Benito, A. M.; Martinez, M. T.; et al. Soluble Self-Aligned Carbon Nanotube/Polyaniline Composites. *Adv. Mater.* **2005**, *17* (3), 278–81.
- (14) Lim, J. A.; Cho, J. H.; Park, Y. D.; Kim, D. H.; Hwang, M.; Cho, K. Solvent effect of inkjet printed source/drain electrodes on electrical properties of polymer thin-film transistors. *Appl. Phys. Lett.* **2006**, *88* (8), 082102.
- (15) Grossiord, N.; Loos, J.; van Laake, L.; et al. High-Conductivity Polymer Nanocomposites Obtained by Tailoring the Characteristics of Carbon Nanotube Fillers. *Adv. Funct. Mater.* **2008**, *18*, 3226–34.
- (16) Geng, H.-Z.; Kim, K. K.; So, K. P.; Lee, Y. S.; Chang, Y.; Lee, Y. H. Effect of acid treatment on carbon nanotube-based flexible transparent conducting films. *J. Am. Chem. Soc.* **2007**, *129* (25), 7758–9.
- (17) Harris, P. J. F. *Carbon Nanotube Science: Synthesis, Properties and Applications*; Cambridge University Press: New York, 2009.
- (18) Meitl, M. A.; Zhou, Y.; Gaur, A.; et al. Solution Casting and Transfer Printing Single-Walled Carbon Nanotube Films. *Nano Lett.* **2004**, *4* (9), 1643–1647.
- (19) Grunlan, J. C.; Mehrabi, A. R.; Bannon, M. V.; Bahr, J. L. Water-Based Single-Walled-Nanotube-Filled Polymer Composite with an Exceptionally Low Percolation Threshold. *Adv. Mater.* **2004**, *16* (2), 150–3.
- (20) Grossiord, N.; Noordover, B. A. J.; Miltner, H. E.; et al. A Latex-Based Route to Disperse Carbon Nanotubes in Poly(2,6-Dimethyl-1,4-Phenylene Ether)/Polystyrene Blends. *Macromol. Mater. Eng.* **2014**, *299*, 228–36.
- (21) Hermant, M.-C.; van der Schoot, P.; Klumperman, B.; Koning, C. E. Probing the cooperative nature of the conductive components in polystyrene/poly(3,4-ethylenedioxothiophene):poly(styrene sulfonate)-single-walled carbon nanotube composites. *ACS Nano* **2010**, *4* (4), 2242–8.
- (22) Yu, J.; Grossiord, N.; Koning, C. E.; Loos, J. Controlling the dispersion of multi-wall carbon nanotubes in aqueous surfactant solution. *Carbon* **2007**, *45* (3), 618–623.
- (23) Kyrylyuk, A. V.; Hermant, M. C.; Schilling, T.; Klumperman, B.; Koning, C. E.; van der Schoot, P. Controlling electrical percolation in multicomponent carbon nanotube dispersions. *Nat. Nanotechnol.* **2011**, *6* (6), 364–9.
- (24) Toolan, D. T. W.; Fujii, S.; Ebbens, S. J.; Nakamura, Y.; Howse, J. R. On the mechanisms of colloidal self-assembly during spin-coating. *Soft Matter* **2014**, *10* (44), 8804–12.
- (25) Pichumani, M.; Bagheri, P.; Poduska, K. M.; González-Viñas, W.; Yethiraj, A. Dynamics, crystallization and structures in colloid spin coating. *Soft Matter* **2013**, *9* (12), 3220.
- (26) Wysocki, A.; Löwen, H. Oscillatory driven colloidal binary mixtures: axial segregation versus laning. *Phys. Rev. E Stat Nonlin Soft Matter Phys.* **2009**, *79*, 041408.
- (27) Santos de Oliveira, I. S.; den Otter, W. K.; Briels, W. J. The origin of flow-induced alignment of spherical colloids in shear-thinning viscoelastic fluids. *J. Chem. Phys.* **2012**, *137* (20), 204908.
- (28) Löwen, H.; Wensink, H. H.; Rex, M.; Tokuyama, M.; Oppenheim, I.; Nishiyama, H. Driven Colloidal Mixtures and Colloidal Liquid Crystals. In *AIP Conference Proceedings*; AIP: St. Louis, MO, 2008; Vol 982, pp 284–288.
- (29) Du, F.; Fischer, J. E.; Winey, K. I. Effect of nanotube alignment on percolation conductivity in carbon nanotube/polymer composites. *Phys. Rev. B: Condens. Matter Mater. Phys.* **2005**, *72* (12), 121404.
- (30) Su, J.; Mirzaee, I.; Gao, F.; et al. Magnetically Assembling Nanoscale Metal Network Into Phase Change Material—Percolation Threshold Reduction in Paraffin Using Magnetically Assembly of Nanowires. *J. Nanotechnol. Eng. Med.* **2014**, *5* (3), 031005.
- (31) Kyrylyuk, A. V.; van der Schoot, P. Continuum percolation of carbon nanotubes in polymeric and colloidal media. *Proc. Natl. Acad. Sci. U. S. A.* **2008**, *105* (24), 8221–6.
- (32) Ha, J.-W.; Park, I. J.; Lee, S.-B. Antireflection Surfaces Prepared from Fluorinated Latex Particles. *Macromolecules* **2008**, *41* (22), 8800–8806.